J. Fluid Mech. (1981), *vol.* 103, *pp.* 389–412
Printed in Great Britain

Effect of rotation on the stability of a doubly diffusive fluid layer

By ARNE J. PEARLSTEIN

Mechanics and Structures Department,
University of California, Los Angeles, California 90024

(Received 13 October 1976 and in revised form 8 November 1979)

The stability of a rotating doubly diffusive fluid is considered. It is shown that (1) a non-rotating layer can be destabilized by rotation, (2) a rotating layer can be destabilized by the addition of a bottom-heavy solute gradient, and (3) under some conditions, three thermal Rayleigh numbers are required to specify linear stability criteria. Numerical results are presented on the basis of which the explanation by Acheson (1979) of the second of these three anomalies can be assessed, and Acheson's explanation is adapted to the two other anomalies.

1. Introduction

Doubly diffusive instabilities have been observed in a variety of fluid systems and have been hypothesized to occur in still others (Turner 1974; Schechter, Velarde & Platten 1974). Among the applications, the following include rotation.

(i) Brakke (1955) observed, and correctly explained, a doubly diffusive instability that occurs when a solution of a slowly diffusing protein is layered over a denser solution of more rapidly diffusing sucrose. Nason *et al.* (1969) demonstrated that this instability can be suppressed by rotation in the ultracentrifuge. This instability, which is deleterious to certain biochemical separations, has also been studied by Sartory (1969), Hsu (1975), Mason (1976), and Halsall & Sartory (1976).

(ii) Stommel & Fedorov (1967), Anati (1972), and Linden (1974) have remarked that the length scales characteristic of doubly diffusive convecting layers in the ocean may be sufficiently large that the Earth's rotation might be important in their formation.

(iii) Ulrich (1972) has recognized that rotation may influence 'semiconvection' in the envelopes and cores of certain stars in which the doubly diffusive character is due to gradients of temperature and mean molecular weight, the gradient of the latter arising from a spatially varying hydrogen–helium ratio.

(iv) Copley (1979, private communication) reports an exploratory experimental attempt to suppress doubly diffusive convection in a solidifying aqueous ammonium chloride solution by employing uniform rigid rotation. This optically transparent aqueous system has been used by Copley *et al.* (1970) to study by analogy the doubly diffusive convection thought to occur in certain casting and crystal growth operations including the production of superalloy single crystal turbine blades (Giamei & Kear 1970).

0022-1120/81/4626-3060 $02.00

(v) Oscillations and layering have been observed by Schaaffs (1975) in a rotating, thermally stratified aqueous solution of ethylene glycol, and Schmitt & Lambert (1979) have experimentally studied the effects of rotation on highly supercritical salt fingers.

(vi) Antoranz & Velarde (1979) have reported numerical calculations of the influence of rigid rotation on the stability of a binary fluid in which (Fickian) diffusive and convective mass transfer are augmented by thermal diffusion (Soret transport). Their goal was to increase the usefulness of the thermogravitational method of measuring the Soret coefficient in liquid systems.

In view of these applications and experimental observations, it is of interest to gain a general understanding of the manner in which rotation affects the hydrodynamic stability of a doubly diffusive fluid. To this end, consideration will be given to the interaction of shear-free, solid-body rotation with the simplest doubly diffusive density distribution (constant vertical gradients of two properties that influence the density) in a fluid layer of infinite horizontal extent.

Three rather surprising results emerge from the linear analysis. Under some conditions, a doubly diffusive layer, stable in the absence of rotation, becomes unstable in the presence of rotation. Furthermore, under other conditions, a linearly stable rotating doubly diffusive layer is destabilized by the addition of heavy solute to the bottom of the layer. Finally, and most surprisingly, under yet another set of conditions, the specification of linear stability criteria requires the calculation of three thermal Rayleigh numbers rather than the usual single value. These possibilities do not appear to have been recognized in previous analytical investigations of the problem by Sani & Scriven (unpublished), Sengupta & Gupta (1971), or Antoranz & Velarde (1979). Only the second of the three anomalies was noticed by Masuda (1978). Since that time, a physical explanation of the second anomaly has been advanced by Acheson (1979). This paper presents information on which Acheson's theory can be assessed and also extends Acheson's explanation to the other two anomalies.

The third anomalous result (requirement for three thermal Rayleigh numbers in order to specify linear stability criteria) has been overlooked not only in all four of the previous investigations of the present problem, but also in a recent study of another convective stability problem (Griffiths 1979).

2. Formulation of the problem

Consider a layer of Boussinesq binary fluid of infinite horizontal extent in the x' and y' directions, confined between parallel stress-free boundaries at $z' = 0$ and $z' = L$ at which the temperatures are T_0 and T_L respectively. The layer rotates uniformly about the z' axis with constant angular velocity Ω. Denote one of the components by A and suppose that the concentration of A is held at C_{A0} and C_{AL} at the lower and upper boundaries, respectively. The equation of state is given by

$$\rho = \bar{\rho}(1 - \alpha_T(T - \bar{T}) + \alpha_C(C_A - \bar{C}_A)),$$

where the mean reference temperature and concentration are defined by $\bar{T} = \frac{1}{2}(T_0 + T_L)$ and $\bar{C}_A = \frac{1}{2}(C_{A0} + C_{AL})$. The non-dimensional linear perturbation equations can then be shown to be

$$(Pr\,\partial/\partial t - \nabla^2)\,\theta - R_T w = 0, \tag{1}$$

$$(Sc\,\partial/\partial t - \nabla^2)\,S - R_S w = 0, \tag{2}$$

$$(\partial/\partial t - \nabla^2)\,\zeta - Ta^{\frac{1}{2}}\,\partial w/\partial z = 0, \tag{3}$$

$$(\partial/\partial t - \nabla^2)\,\nabla^2 w + Ta^{\frac{1}{2}}\,\partial\zeta/\partial z - \nabla_1^2\theta - \nabla_1^2 S = 0, \tag{4}$$

where ζ is the vertical vorticity and $R_T = \alpha_T g L^3(T_0 - T_L)/\kappa\nu$, $R_S = \alpha_C g L^3(C_{AL} - C_{A0})/D\nu$, $Ta = 4\Omega^2 L^4/\nu^2$, $Pr = \nu/\kappa$, and $Sc = \nu/D$ are the thermal Rayleigh, solute Rayleigh, Taylor, Prandtl, and Schmidt numbers, respectively. It is also required that the conditions

$$w = \partial^2 w/\partial z^2 = \partial\zeta/\partial z = \theta = S = 0, \tag{5}$$

be satisfied at the stress-free boundaries $z = 0$ and $z = 1$. The horizontal Laplacian $\nabla_1^2 = \partial^2/\partial x^2 + \partial^2/\partial y^2$ has been introduced, and D, κ, ν and g are the diffusivity of A, the thermal diffusivity, the kinematic viscosity and the gravitational acceleration, respectively.

3. Linear stability analysis

To examine the stability of (1)–(5), solutions of the form

$$\phi(x, y, z, t) = \phi_0 \sin \pi z \exp(ik_x x + ik_y y + \sigma t),$$

where ϕ is any disturbance quantity, are chosen. (Inclusion of solutions with vertical dependence $\sin n\pi z$, $n > 1$, does not alter the linear stability criteria calculated here.) Substitution into (1)–(5) leads to the relationship

$$(y(y+\sigma)^2 + \pi^2 Ta)\,(y + \sigma Pr)\,(y + \sigma Sc) - k^2(y+\sigma)\,(R_T(y + \sigma Sc) + R_S(y + \sigma Pr)) = 0, \tag{6}$$

where $y = \pi^2 + k^2$ and $k^2 = k_x^2 + k_y^2$. The two Rayleigh numbers R_T and R_S have been chosen to make the mathematical problem (6) invariant with respect to the interchange ($R_T \leftrightarrow R_S$, $Pr \leftrightarrow Sc$). For the same reason, the parameters Pr and Sc have been used instead of Pr and $\tau = Pr/Sc$. (For an isothermal ternary fluid, one need only replace R_T and Pr by a second solute Rayleigh number and a second Schmidt number, respectively.)

One of the ways in which (6) may be used to examine the stability of a fluid configuration will now be discussed. The parameters k, Ta, Pr, Sc and one of the Rayleigh numbers (say R_S) are taken as given. The other Rayleigh number (R_T) is considered to be a free parameter that is varied until a neutral (marginal) solution of (1)–(5) with $\mathrm{Re}(\sigma) = 0$ is obtained. To do this, we recast (6) as

$$R_T = -\frac{y + \sigma Pr}{y + \sigma Sc} R_S + \left(y(y+\sigma)\,(y+\sigma Pr) + \frac{\pi^2 Ta(y+\sigma Pr)}{y+\sigma}\right) \Big/ k^2, \tag{7}$$

and then set the real part of σ equal to zero (let $\sigma = i\omega$). After complex quantities are cleared from the denominators, (7) yields

$$R_T = -\frac{y^2 + \omega^2 PrSc}{y^2 + \omega^2 Sc^2} R_S + \left(y^3 - y\omega^2 Pr + \frac{\pi^2 Ta(y^2 + \omega^2 Pr)}{y^2 + \omega^2}\right) \Big/ k^2 + i\omega y M, \tag{8}$$

with

$$M = \frac{Sc - Pr}{y^2 + \omega^2 Sc^2} R_S + \frac{\pi^2 Ta(Pr - 1)}{k^2(y^2 + \omega^2)} + \frac{y(1 + Pr)}{k^2}. \tag{9}$$

The physical quantity R_T must be real, so that (8) implies that either $\omega = 0$ or $M = 0$.

For $\omega = 0$, (8) gives

$$R_T = R_T^s = -R_s + (y^3 + \pi^2 Ta)/k^2, \tag{10}$$

so that for steady neutral solutions, R_T is a single-valued function of k with a unique minimum at $k = k^s_{\min}$ satisfying (A 2a) of the appendix. An 'effective Rayleigh number' $R_e = R_T + R_S$ may be defined, and the linear stability of a rotating doubly diffusive fluid layer with respect to the onset of steady convection is seen to be determined by whether or not the sum $R_T + R_S$ exceeds

$$R^s_{e,\min} = 3y_s^2(Ta), \tag{11}$$

where $y_s = (k^s_{\min})^2 + \pi^2$. As might have been expected, this steady result is independent of the transport properties Pr and Sc.

For oscillatory ($\omega \neq 0$) neutral solutions of (1)–(5), (8) requires $M = 0$. The vanishing of M provides a dispersion relation of the form

$$\delta\omega^4 + \beta\omega^2 + \gamma = 0 \tag{12}$$

with

$$\delta = y(1+Pr)\,Sc^2, \tag{13a}$$

$$\beta = y^3(1+Pr)\,(1+Sc^2) + \pi^2 Ta(Pr-1)\,Sc^2 - k^2 R_S(Pr - Sc), \tag{13b}$$

$$\gamma = y^2(y^3(1+Pr) + \pi^2 Ta(Pr-1) - k^2 R_S(Pr - Sc)). \tag{13c}$$

Because oscillatory solutions are possible both in the non-rotating doubly diffusive case ($Ta = 0$) with frequency given by

$$\omega^2 = \frac{k^2 R_S(Pr - Sc) - y^3(1+Pr)}{y(1+Pr)\,Sc^2}, \tag{14a}$$

and in the rotating singly diffusive case ($Pr = Sc$) with frequency given by

$$\omega^2 = \frac{\pi^2 Ta(1-Pr) - y^3(1+Pr)}{y(1+Pr)}, \tag{14b}$$

(12) is a quadratic in ω^2 and can give rise to more than one positive value of ω^2 for fixed k, R_S, Ta, Pr, and Sc. This has important implications for the linear stability of a rotating doubly diffusive fluid, as will become clear in § 3.2. Furthermore, the possibility of multiple real frequencies, and hence multiple oscillatory neutral solutions, occurs in other convective stability problems, as will be discussed in § 4. Thus, it is worthwhile to establish necessary conditions for the existence of two oscillatory neutral solutions. From Descartes' rule of signs, in order for (12) to have two positive roots, it is necessary that $\beta < 0$ and $\gamma > 0$, from which it follows, using (13b, c), that

$$y^3(1+Pr)\,(1+Sc^2) + \pi^2 Ta(Pr-1)\,Sc^2 < k^2 R_S(Pr - Sc) < y^3(1+Pr) + \pi^2 Ta(Pr-1).$$

Therefore,

$$0 < y^3(1+Pr)\,Sc^2 < \pi^2 Ta(Pr-1)\,(1-Sc^2),$$

which is equivalent to requiring that one of the conditions

$$Pr > 1 > Sc \quad \text{or} \quad Sc > 1 > Pr \tag{15a, b}$$

be satisfied.

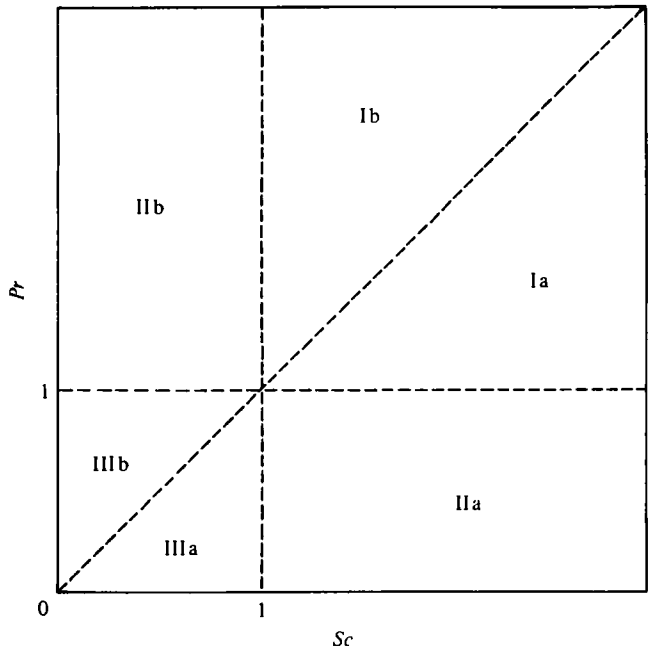

FIGURE 1. Regions of the quarterplane in which the Prandtl and Schmidt numbers are both non-negative.

It is convenient to divide the portion of the Pr–Sc plane in which these two 'transport numbers' are non-negative into six regions, as shown in figure 1. The methods used and results obtained in regions Ia and Ib, IIa and IIb, and IIIa and IIIb are described in § 3.1, 3.2, and 3.3, respectively. Some new results for the singly diffusive case ($Pr = Sc$), previously discussed by Chandrasekhar (1961, chapter III), are presented in the appendix.

3.1. *Regions I a and I b*

Because neither of (15a, b) is satisfied in these regions, no more than one oscillatory neutral solution can exist for each wavenumber k, a conclusion reached by Sani & Scriven for the case $R_S < 0$. We remember that in a singly diffusive stratified rotating layer, linear theory predicts that the stationary mode is the preferred mode of instability if the Prandtl (or Schmidt) number exceeds $Pr^* = 0{\cdot}6766\ldots$, at which value the denominator of (A 4) of the appendix vanishes. Thus in a rotating doubly diffusive fluid with both Pr and Sc greater than unity, the oscillatory instability associated with inertial wave propagation in a singly diffusive stratified rotating fluid should not be expected to occur.

Important information about the neutral curves in the $R_T - k$ plane may be deduced by locating the bifurcation points at which the steady and oscillatory neutral curves join. These must occur on the steady R_T^s–k curve at wavenumbers k_b for which $\omega = 0$ is a root of (12). Thus $\gamma(k_b) = 0$, or equivalently

$$k_b^6 + 3\pi^2 k_b^4 + (3\pi^4 - R_S(Pr - Sc)/(1+Pr))\, k_b^2 + \pi^6 + \pi^2 Ta(Pr-1)/(1+Pr) = 0, \quad (16)$$

so that for $Pr > 1$ the left hand side of (16) is a cubic polynomial in k_b^2 with either zero

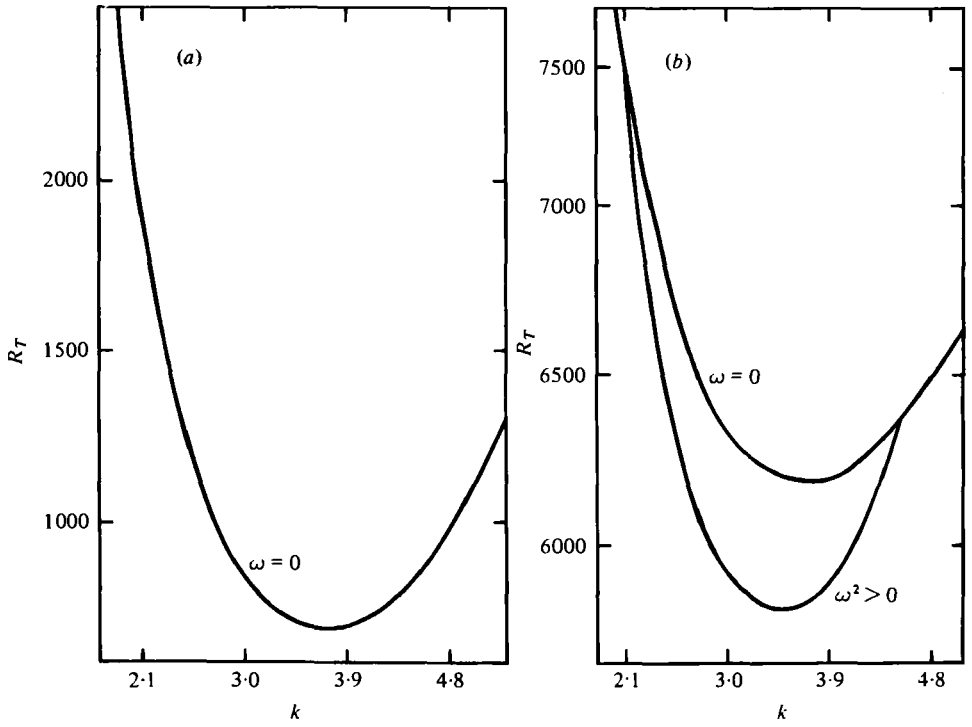

FIGURE 2. Curves of neutral stability in the R_T–k plane. (*a*) $Pr = 7$, $Sc = 700$, $Ta = 1000$, $R_S = 1000$. (*b*) $Pr = 2$, $Sc = 3$, $Ta = 1000$, $R_S = -4500$.

or two sign changes. Hence, by Descartes' rule of signs, either there are no bifurcation points or there are two. Typical neutral curves in the R_T–k plane are shown in figures 2(*a*) and (*b*). These neutral curves, like those for the rotating case (Chandrasekhar 1961, fig. 27) and the non-rotating doubly diffusive case, are connected in a topological sense (Apostol 1957, §8.11). This connectedness allows the linear stability criteria to be expressed in terms of a *single* 'critical thermal Rayleigh number' R_T^c, below which a configuration is linearly stable and above which it is definitely unstable. The numerical determination of R_T^c proceeds as follows. One first determines the number of positive solutions k_b of (16). If there are none, then no oscillatory instability is possible and R_T^c is given by (A 3*a*). If there are two, then the minimum (over k) of (8) with ω^2 given by (12) is compared with $R_{T,\min}^s$ given by (A 3*a*) and the smaller value is R_T^c, corresponding to the critical wavenumber k_c.

Results obtained according to this procedure for the case of salt water, $Pr = 7$, $Sc = 700$, are shown in figure 3 and table 1. The lowest locus in figure 3 is the non-rotating case $Ta = 0$, for which (8) and (14*a*) predict the onset of oscillatory motion to occur at

$$R_{T,\min}^o = -\frac{Pr^2(1+Sc)}{Sc^2(1+Pr)}R_S + \frac{27\pi^4(Sc+Pr)(1+Sc)}{4Sc^2}.$$

For $Ta = 0$, the minimum thermal Rayleigh number for stationary convection is

$$R_{T,\min}^s = -R_S + \tfrac{27}{4}\pi^4,$$

	Ta = 0		Ta = 10^2			Ta = 10^3			Ta = 10^4			
R_S	R_T^c	k_c	R_T^c	ΔR_T^c	k_c	R_T^c	ΔR_T^c	k_c	R_T^c	ΔR_T^c	k_c	Mode of instability
10^4	−9342·5	2·221	−9173·7	168·78	2·594	−8323·9	1018·6	3·710	−4622·9	4719·6	5·698	stat.
10^3	−342·49	2·221	−173·71	168·78	2·594	676·12	1018·6	3·710	4377·1	4719·6	5·698	stat.
0	657·51	2·221	826·29	168·78	2·594	1676·1	1018·6	3·710	5377·1	4719·6	5·698	stat.
-10^3	673·80	2·221	844·45	170·66	2·594	1702·9	1029·1	3·709	5440·0	4766·2	5·695	osc.
-10^4	752·66	2·221	926·62	173·96	2·600	1790·3	1037·7	3·719	5530·6	4777·9	5·700	osc.
-10^5	1541·3	2·221	1746·8	205·50	2·664	2661·2	1119·9	3·807	6435·5	4894·2	5·747	osc.

TABLE 1. Values of the critical thermal Rayleigh number R_T^c and critical wavenumber k_c for various values of the Taylor number and solute Rayleigh number. For the rotating cases (Ta non-zero), the absolute stabilization $\Delta R_T^c = R_T^c(Ta) - R_T^c(0)$ due to rotation is also shown. The mode of instability depends only on R_S in the cases shown here and appears in the rightmost column. The results are for salt water ($Pr = 7$, $Sc = 700$).

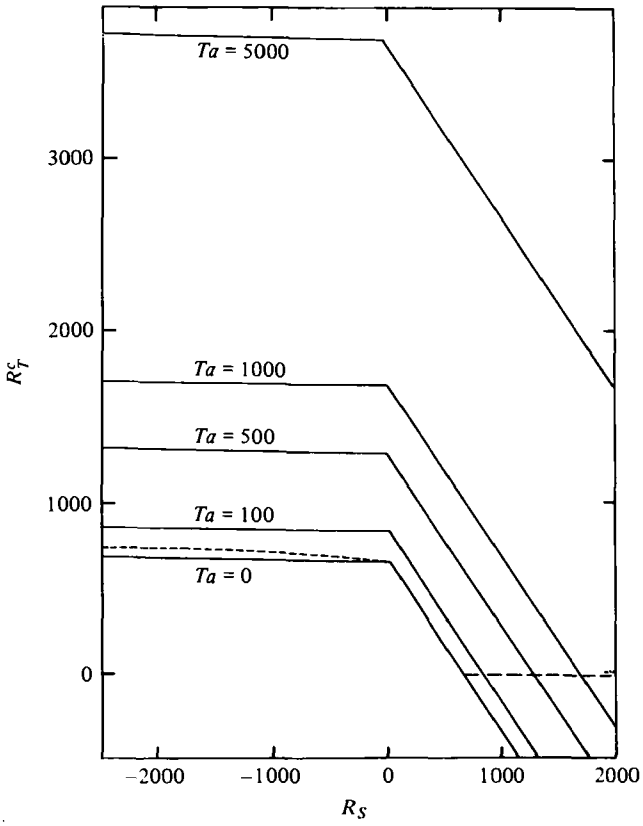

FIGURE 3. Variation of the critical Rayleigh number, R_T^c, with R_S for salt water ($Pr = 7, Sc = 700$). The portion of each stability boundary lying to the left of the discontinuity in slope corresponds to oscillatory onset ($\omega^2 > 0$), while to the right, the onset is of the steady type ($\omega = 0$). The 'fingering' line (— — —) is $R_T Sc + R_S Pr = 0$, and the 'diffusive' curve (– – –) is calculated from a corrected version of equation 3.3 of Baines & Gill (1969).

so that in the non-rotating case, R_T^c is a piecewise linear function of R_S. At

$$\bar{R}_S = \frac{27\pi^4(1+Pr)}{4(Pr-Sc)},$$

the slope of the R_T^c–R_S plot changes, as does the preferred mode of instability. From figure 3, one may observe that the principal effect of rotation is to stabilize the fluid against convection. Aside from this stabilization, the R_T^c–R_S plots are virtually unaffected. In the region of steady onset (R_S generally positive), the linearity is retained exactly, according to (10). In the region of oscillatory onset, the deviations from linearity are very slight. Also, the solute Rayleigh number $\bar{R}_S$ at which the preferred mode of instability changes is affected very little. From table 1, it may be seen that k_c is independent of R_S in the region of stationary onset ($R_S > \bar{R}_S$) and varies slowly with R_S for $R_S < \bar{R}_S$. For salt water, k_c depends primarily on Ta. Furthermore, for $Ta = 10^3$ or 10^4, k_c can be shown to have a minimum near $\bar{R}_S$. In fact, the variation of k_c with $\bar{R}_S$ can be not only non-monotonic but also discontinuous. This behaviour is more pronounced for other combinations of Pr and Sc, as will be seen in § 3.2.

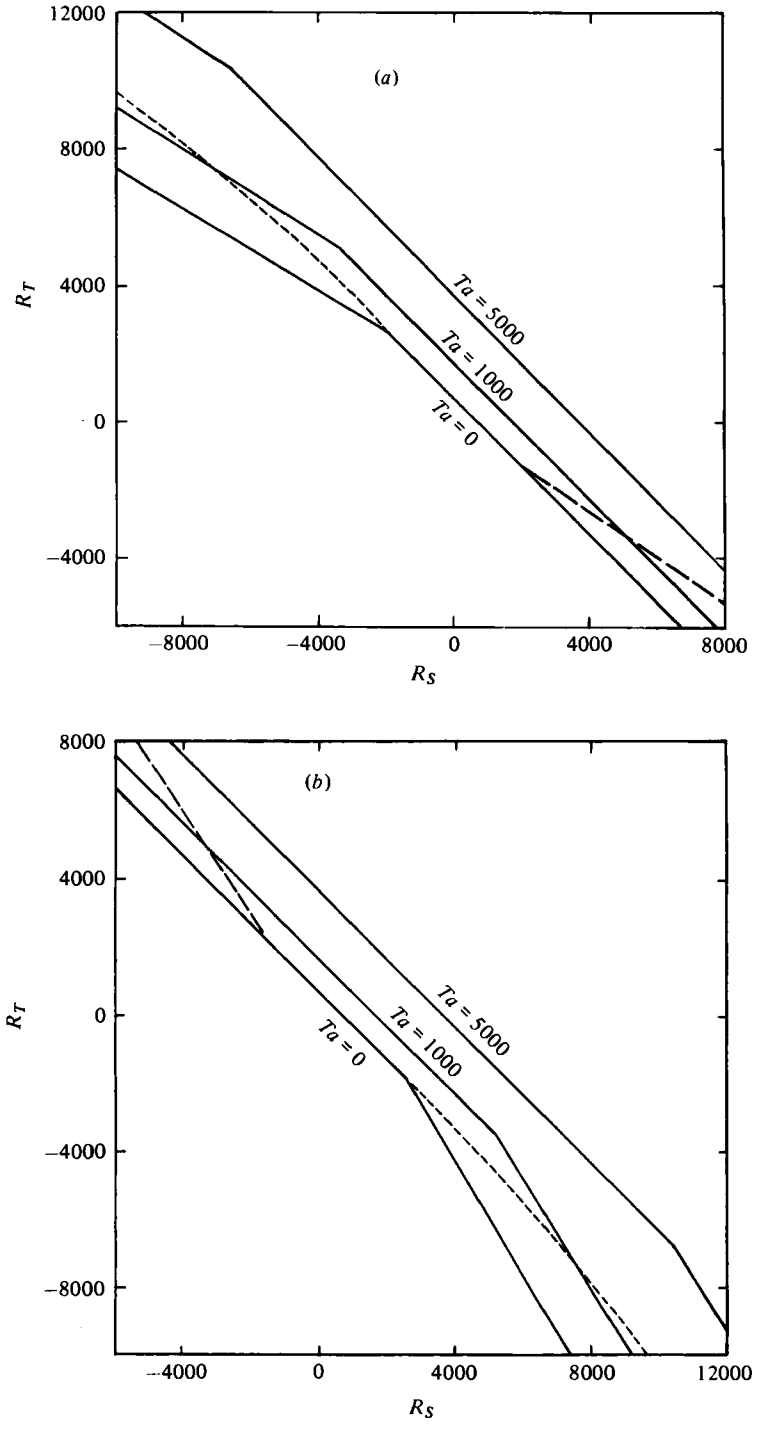

FIGURE 4. Variation of R_T^c with R_S for several Taylor numbers. (*a*) $Pr = 2$, $Sc = 3$. Oscillatory onset to the left of each slope discontinuity, and steady onset to the right. (*b*) $Pr = 3$, $Sc = 2$. Steady onset to the left of each slope discontinuity, oscillatory onset to the right. ———, 'Fingering' line; – – –, 'diffusive' curve.

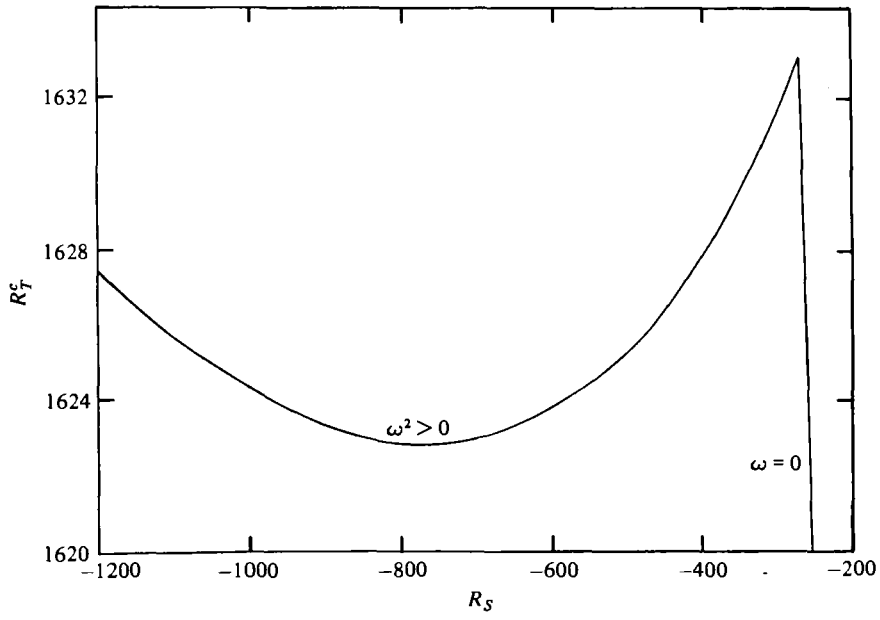

FIGURE 5. Destabilization by addition of a bottom, heavy-solute gradient for $Pr = 0{\cdot}2$, $Sc = 1{\cdot}2$, $Ta = 600$.

Figure 3 also shows that rotation inhibits the steady and oscillatory motions to very nearly the same extent. Closer inspection (see table 1) shows that the absolute increase in R_T^c due to rotation is slightly greater at large negative solute Rayleigh numbers, for which instability sets in as oscillations, than at large positive values of R_S, for which the onset of steady convection is preferred. The difference in stabilization, small for salt water, is vividly illustrated in figure 4(*a*) for $Pr = 2, Sc = 3$ (region I*a*). Symmetrical results for $Pr = 3, Sc = 2$ (region I*b*) are shown in figure 4(*b*). The variation of $\bar{R}_S$ with Ta is more readily apparent in these cases of smaller and more nearly equal Pr and Sc.

The inhibition by rotation of the onset of stationary convection is a direct consequence of the Taylor–Proudman theorem. That oscillatory motion is even more strongly inhibited is at first surprising. The explanation is thought to lie in the fact that, in a thermally stratified fluid with $R_S = 0$, oscillatory instability is not possible if $Pr > 1$. Thus it seems logical that in a doubly diffusive fluid with both Pr and Sc greater than one, oscillatory doubly diffusive instability will be prohibited at Taylor numbers sufficiently large to dominate the flow. The behaviour shown in figures 3, 4(*a*) and (*b*), and table 1 is certainly consistent with this conjecture.

3.2(*a*). *Region II a*

In this part of the parameter space ($Pr < 1 < Sc$), a rotating doubly diffusive layer can be destabilized by decreasing R_S, for example, by adding heavy solute to the bottom. The destabilization manifests itself as a minimum in the R_T–R_S plot, as shown in figure 5. For R_S sufficiently negative, decreasing R_S stabilizes the layer, as expected. Similarly, for R_S sufficiently large, further increases in R_S destabilize the layer. As seen in figure 5, however, for certain combinations of Pr, Sc, and Ta there

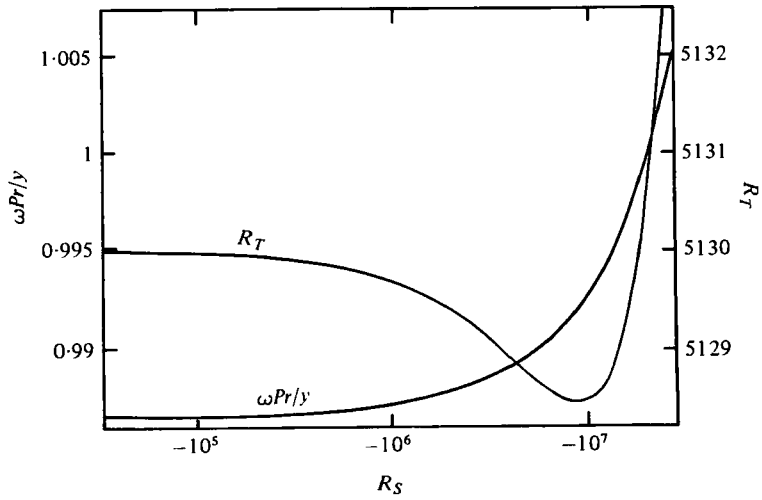

FIGURE 6. Variation of R_T and $\omega Pr/y$ with R_S for $Pr = 0{\cdot}025$, $Sc = 101$, $Ta = 4 \times 10^6$.

is some intermediate range of R_S in which the layer is destabilized by decreasing R_S and stabilized by increasing R_S. This result has also been obtained by Masuda (1978), but until the work of Acheson (1979), no physical explanation was available.

Acheson notes that in a thermally stratified rotating fluid ($R_S = 0$), with $Pr < 1$, the basic overstability mechanism is associated with inertial wave propagation. The frequency is determined by the Taylor number. For Sc very large in a doubly diffusive rotating fluid, diffusion of solute is so slow that substantial changes in the bobbing frequency can be produced by changes in R_S that have little stabilizing effect *via* solute diffusion. Thus, the frequency can be 'tuned' by adjusting R_S. If the frequency is too small, a bobbing parcel will always remain in approximate thermal equilibrium with its environment. If the frequency is too high, no significant heat transfer will occur into or out of the parcel in the first place. In either extreme, the basic overstability mechanism is operating at less than optimal efficiency. At some intermediate frequency, however, the maximum efficiency is achieved, and overstable oscillations set in at a lower value of R_T than is possible for larger or smaller frequencies.

To make this quantitative, Acheson does the following. The temperature difference between a parcel bobbing with frequency ω and its surroundings as it passes through its equilibrium position is

$$\Delta T = -h\frac{dT}{dz}\frac{\omega Pr\, y}{\omega^2 Pr^2 + y^2} = -h\frac{dT}{dz}\frac{\omega Pr/y}{(\omega Pr/y)^2 + 1}, \tag{17}$$

where h is the displacement amplitude, dT/dz is the vertical temperature gradient, and $y = \pi^2 + k^2$ is the square of the total wavenumber. This temperature difference is maximized when $\omega Pr/y$ is unity, and hence Acheson's analysis predicts that when Sc is large, the local minimum in the R_T–R_S plot will occur when $\omega Pr/y = 1$. Figure 6 shows plots of $\omega Pr/y$ and R_T *versus* R_S for $Pr = 0{\cdot}025$, $Sc = 101$, and $Ta = 4 \times 10^6$. It is seen that $\omega Pr/y = 0{\cdot}993$ at $R_S = -10^7$ (approximately the value of R_S that minimizes R_T), and although $\omega Pr/y$ is only slightly less than that value for larger (less negative) values of R_S, it is nonetheless clear from figure 6 that the destabilization is associated with a monotonically increasing $\omega Pr/y$, just as predicted by Acheson.

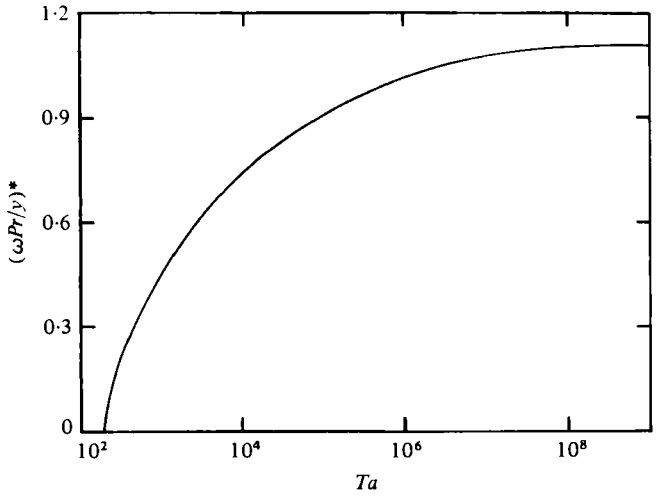

FIGURE 7. Variation of $(\omega Pr/y)^*$ with Ta for $Pr = 0{\cdot}5$, $Sc = 101$.

Indeed, after much algebra,† it can be shown that at the value of R_S which (locally) minimizes R_T the ratio $\omega Pr/y$ is given by

$$(\omega Pr/y)^* \equiv \left.\frac{\omega Pr}{y}\right|_{\partial R_T/\partial k = \partial R_T/\partial R_S = 0} = \left[\frac{2z_0 - 3 + 3Pr^2(1-z_0)}{z_0}\right]^{\frac{1}{2}}, \tag{18a}$$

where z_0 is the largest real root of $z_0(2z_0-3)^2 + B = 0$ and

$$B = \frac{Ta(Sc-1)\,Pr^2}{(1-Pr^2)\,(Sc+1)\,\pi^4}. \tag{18b}$$

This allowed the computation of $(\omega Pr/y)^*$ for a large number of combinations of Pr, Sc, and Ta. Results for $Pr = 0{\cdot}5$ and $Sc = 101$ are shown in figure 7, wherein it is seen that $(\omega Pr/y)^*$ is always less than $\sqrt{2}$, and that $(\omega Pr/y)^*$ approaches $(2-3Pr^2)^{\frac{1}{2}}$ as Ta (and hence B) become large. In fact, for $Pr < \frac{1}{3}$, there is, in addition to the lower bound on Ta for which destabilization (existence of a minimum in the R_T–R_S curve) is possible (shown in figure 7 at $Ta \approx 200$), also an upper bound on the range of Ta for which destabilization occurs. Thus, in practice, the largest value of $(\omega Pr/y)^*$ is less than $\sqrt{2}$.

For $Pr = 0{\cdot}75$, $Sc = 1{\cdot}75$, and various values of Ta, figure 8 shows the variation of k_c with R_S. At $R_S = \bar{R}_S$, the oscillatory and stationary neutral curves have their minima at the same R_T. If these minima occur at different wavenumbers, a discontinuous k_c–R_S plot results. Such an effect was noted in § 3.1 for salt water and is much more evident here.

Finally, we take note of the neutral curve shown in figure 9 for $Pr = 0{\cdot}1$, $Sc = 10$, $Ta = 1000$, and $R_S = 1600$, in which the oscillatory neutral curve bifurcates from the stationary neutral curve at a small wavenumber ($k \simeq 2$) and then crosses the stationary neutral curve at $k \simeq 2{\cdot}3$. This crossing is not a bifurcation and the frequency of the oscillatory neutral disturbance there is not zero. Even more interesting neutral curves will be discussed in the next section.

† The details of which are available on request from the author.

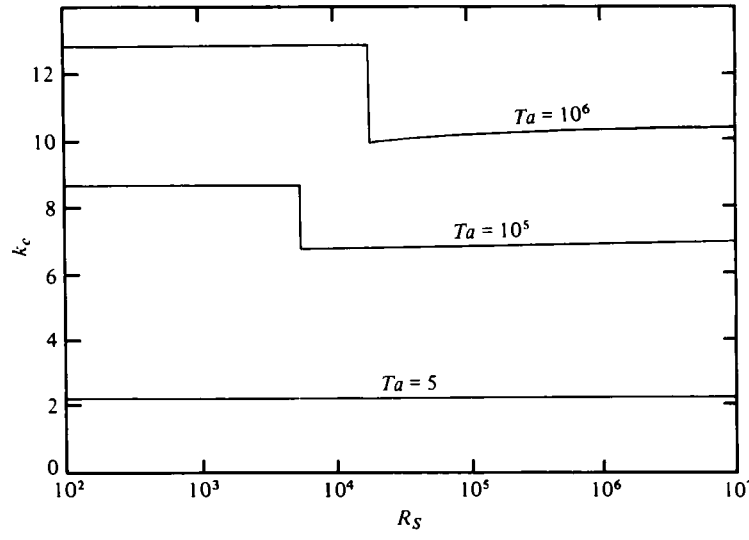

FIGURE 8. Variation of the critical wavenumber k_c with R_S for $Pr = 0{\cdot}75$, $Sc = 1{\cdot}75$.

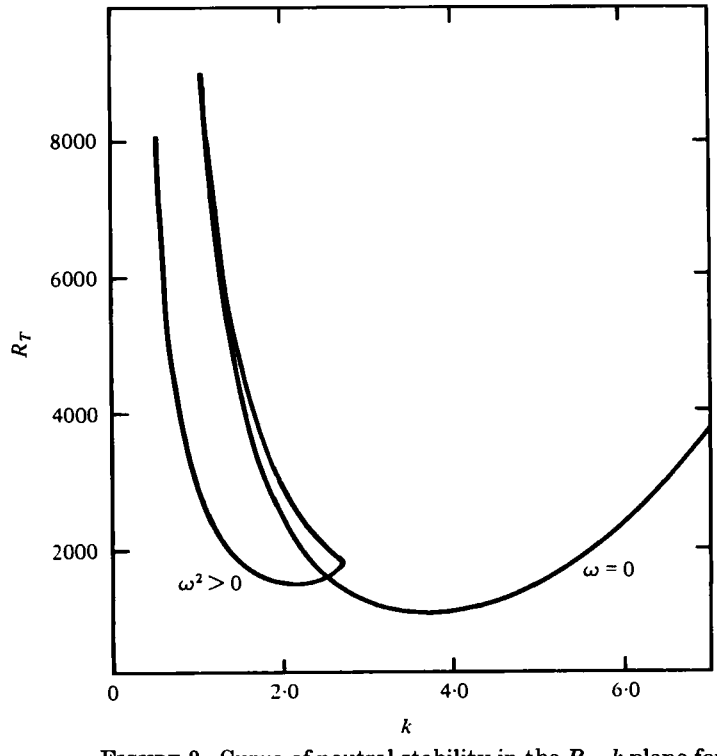

FIGURE 9. Curve of neutral stability in the R_T–k plane for $Pr = 0{\cdot}1$, $Sc = 10$, $Ta = 1000$, $R_S = 1600$.

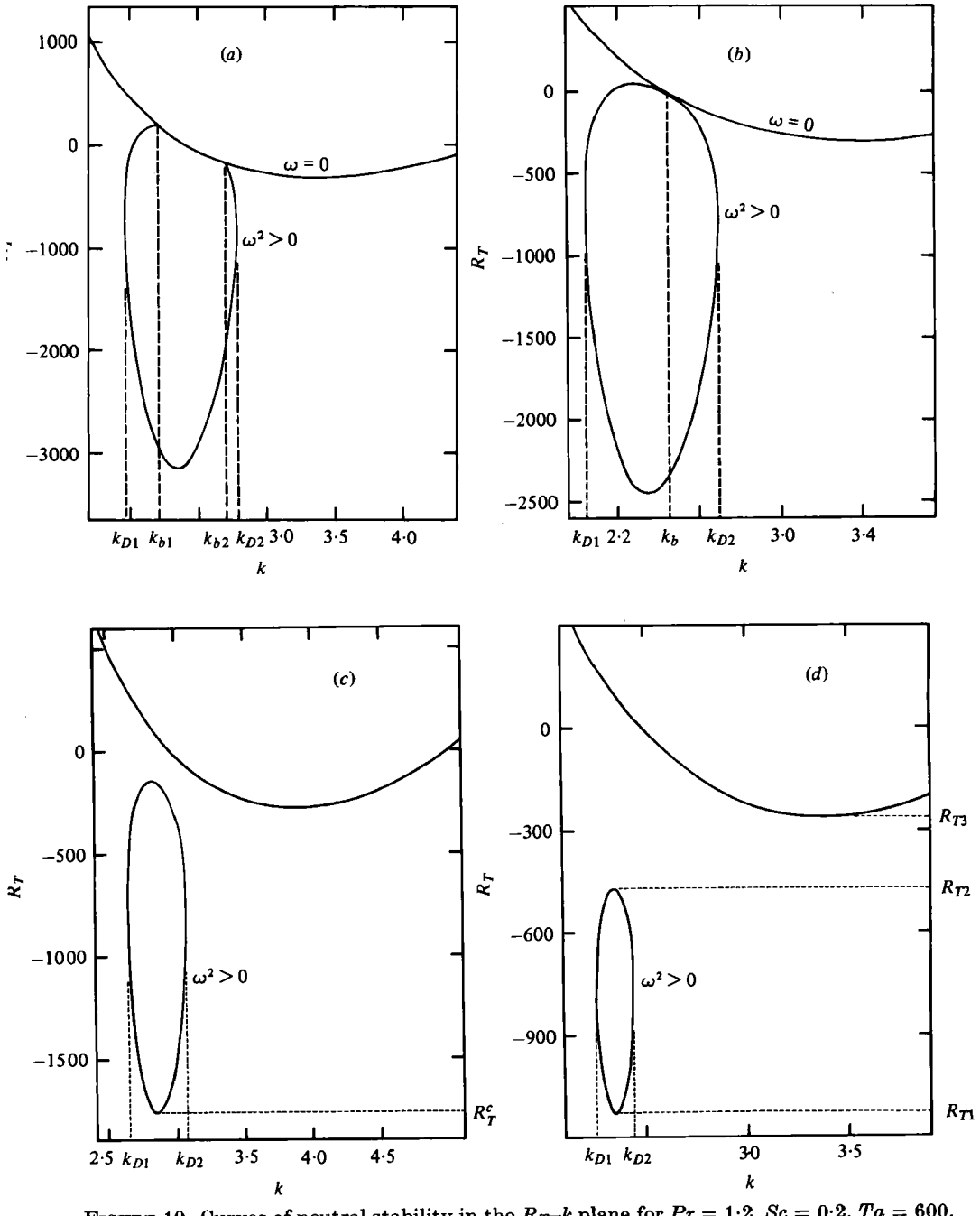

FIGURE 10. Curves of neutral stability in the R_T–k plane for $Pr = 1{\cdot}2$, $Sc = 0{\cdot}2$, $Ta = 600$. (*a*) $R_S = 1690$. (*b*) $R_S = 1662{\cdot}83$. (*c*) $R_S = 1640$. (*d*) $R_S = 1625$.

3.2 (*b*).

For $Pr > 1 > Sc$, examination of (16) shows that neutral curves with zero or two bifurcation points are possible, as in regions I*a* and I*b*. The crucial difference is that in region II*b*, the absence of bifurcation points in the R_T–k plane does not imply the absence of oscillatory neutral solutions, as will now be demonstrated.

Figures 10(*a*)–(*c*) show successive neutral curves for decreasing values of R_S with Ta, Pr and Sc fixed. The neutral curve of figure 10(*a*) is similar to some that occur in regions I*a* and I*b*, except that a pinching of the oscillatory part has given rise to two oscillatory neutral solutions for some wavenumbers, an impossibility in regions I*a*, I*b*, and II*a*, according to (15*a*, *b*). In figure 10(*b*), the pinching has progressed so far that the two distinct bifurcation points, k_{b1} and k_{b2}, at which the oscillatory and steady portions of the neutral curve of figure 10(*a*) are connected, have coalesced to a point of tangency at k_b. At an even smaller R_S, (figure 10(*c*)), a fully disconnected situation has been achieved. The minimum and maximum wavenumbers for oscillatory neutral solutions, k_{D1} and k_{D2}, can be determined by the condition that the discriminant of (12) vanishes for such wavenumbers, i.e. $\beta^2 - 4\delta\gamma = 0$.

Thus far, the linear stability question can still be answered in terms of a single critical thermal Rayleigh number (figures 10(*a*)–(*c*)). However, a further reduction in R_S may give rise to the situation depicted in figure 10(*d*). Here it is seen that there is a range of thermal Rayleigh numbers $R_{T2} < R_T < R_{T3}$ for which all solutions, oscillatory or steady, of the linear disturbance equations are stable at any wavenumber. Thus, the linear stability criteria involve three values of R_T and may be stated as follows. For $R_T < R_{T1}$, and $R_{T2} < R_T < R_{T3}$, the layer is linearly stable. For $R_{T1} < R_T < R_{T2}$, and $R_T > R_{T3}$, the layer is unstable. In such a case, two interesting experimental results are predicted by the linear analysis for a fluid with a positive coefficient of thermal expansivity α_T:

(i) for $R_{T2} < R_T < R_{T3}$, cooling the bottom of the layer may bring about the onset of motion, and

(ii) convection in an overstable layer with $R_{T1} < R_T < R_{T2}$ may be suppressed by heating the bottom.

As R_S is decreased further beyond the value corresponding to figure 10(*d*), the closed oscillatory neutral curve eventually shrinks to a point and disappears.

In figure 11, neutral stability boundaries are given for the case $Pr = 1{\cdot}2$, $Sc = 0{\cdot}2$. The $Ta = 0$ locus is, as usual, a piecewise linear function of R_S. For non-zero Taylor numbers, the oscillatory part of each locus has a certain amount of curvature. For $Ta < 180{\cdot}8198\ldots$, the doubly diffusive effects dominate the layer and the R_T–R_S plots are of the familiar single-valued type. Linear stability is determined by whether or not R_T exceeds the critical value R_T^c. For intermediate rotation rates

$$(180{\cdot}8198\ldots < Ta < 3114{\cdot}560\ldots),$$

Coriolis and doubly diffusive effects are of comparable importance. Their interaction is responsible for the neutral stability curve shown in figure 10(*d*) and the subsequent need to specify linear stability criteria in terms of three thermal Rayleigh numbers. The region near the intersection of the steady and oscillatory portions of the R_T–R_S curve for $Ta = 600$ is shown in expanded form in figure 12. If the layer rotates sufficiently fast ($Ta > 3114{\cdot}560\ldots$), the Coriolis force is dominant, and the locus in the R_T–R_S plane is again single-valued for these values of Pr and Sc.

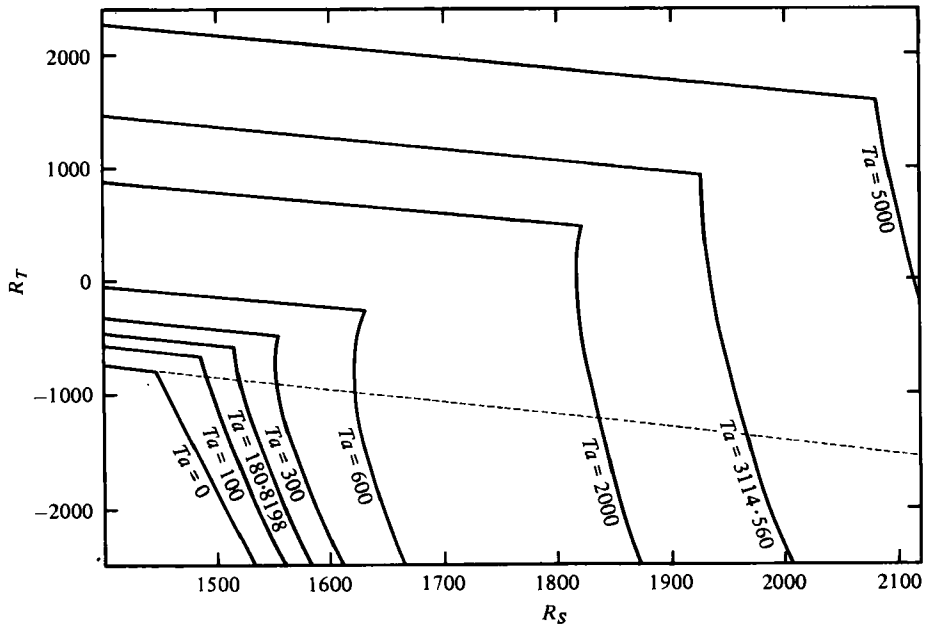

FIGURE 11. R_T–R_S plots for $Pr = 1{\cdot}2$, $Sc = 0{\cdot}2$ for various Taylor numbers. The straight, and nearly horizontal, portion of each stability boundary corresponds to steady onset, while the portion below the slope discontinuity is characterized by $\omega^2 > 0$. ---, 'Diffusive' curve. The 'fingering' line appears off of the diagram for $R_S < 0$.

Figure 13 shows, for various Pr and Sc, the range of Ta for which multivalued plots like figure 12 can occur (in the region above a curve with given Sc). For some Pr and Sc, multivalued R_T–R_S plots are not possible at any Ta, e.g. $Pr = 1{\cdot}05$, $Sc = 0{\cdot}2$ and $Pr = 2$, $Sc = 0{\cdot}8$. For some Pr and Sc, such plots are possible for all sufficiently large values of Ta, with no upper limit. Examples are $Pr = 100$, $Sc = 0{\cdot}5$ ($Ta > 200$), and $Pr = 3$, $Sc = 0{\cdot}8$ ($Ta > 5 \times 10^6$). For other values of Pr and Sc, multivaluedness occurs for a finite range of Taylor numbers, as for the case shown in figure 11.

As formulated in § 2, the present problem is invariant with respect to the interchange ($R_T \leftrightarrow R_S, Pr \leftrightarrow Sc$). Thus, R_T–R_S plots in region IIb may be obtained from the corresponding R_T–R_S plots in region IIa. One may note this from a comparison of the R_T–R_S plots of figure 5 ($Pr = 0{\cdot}2$, $Sc = 1{\cdot}2$, $Ta = 600$) and figure 12 ($Pr = 1{\cdot}2$, $Sc = 0{\cdot}2$, $Ta = 600$). The symmetry is clear, as is the physical explanation which simply requires the interchange of R_T and R_S in the explanation put forward in § 3.2a.

It is also evident from this symmetry that the existence of conditions in region IIb for which three thermal Rayleigh numbers are required to specify linear stability (and indeed, the existence of the disconnected neutral curves) follows directly from the existence of conditions in region IIa for which the R_T–R_S plot has a local minimum.

3.3. *Regions IIIa and IIIb*

For combinations of Pr and Sc in these regions, neither of (15a, b) is satisfied, so again no more than one oscillatory neutral solution per wavenumber is possible. Also, the left-hand side of (16), considered as a cubic polynomial in k_b^2, can have zero, one, or

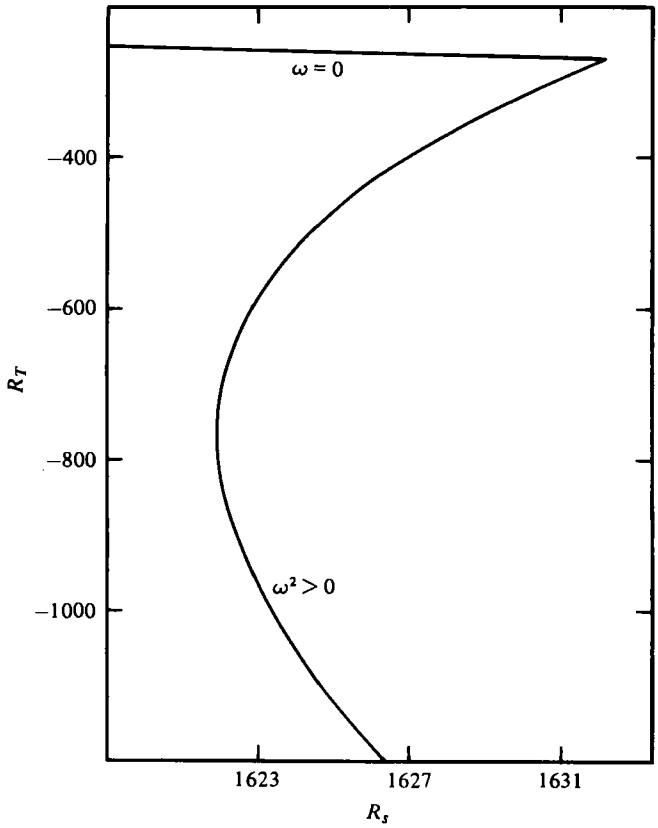

FIGURE 12. Multivalued R_T–R_S plot for $Pr = 1{\cdot}2$, $Sc = 0{\cdot}2$, $Ta = 600$.

two sign changes. Therefore, neutral curves with zero, one, or two bifurcation points are possible. The three possibilities are shown in figures 2(*a*) and (*b*), and figures 27 of Chandrasekhar (1961). The neutral curves are again connected, so that the linear stability analysis need only provide a critical value of R_T and the associated k_c. Numerical results are shown in figure 14 for the case $Pr = 0{\cdot}2$, $Sc = 0{\cdot}5$.

A most striking feature is the crossing of the $Ta = 0$ and $Ta = 10^3$ loci. For example, a non-rotating layer stratified according to $R_T = 3500$, $R_S = -4500$ is predicted by linear theory to be stable, but when rotating with $Ta = 10^3$, it is unstable. The basic thermal and compositional stratifications are identical in the presence and absence of rotation so that this apparent destabilization is not produced by a rotation induced density rearrangement, such as by baro-diffusion.

This result differs from the destabilization by rotation predicted for the onset of thermal convection in certain viscoelastic fluids by Takashima (1970) and Bhatia & Steiner (1972). In those studies, R_T asymptotically approaches, from above, a limiting value as Ta approaches infinity. In the rotating doubly diffusive case, there is no such limit and R_T increases without bound for Ta sufficiently large. Thus, the destabilization appears as a minimum in the R_T–Ta curve, as shown in figure 15.

The existence of such a minimum suggests that this destabilization by rotation may have a physical basis similar to that proposed by Acheson (1979) to explain the

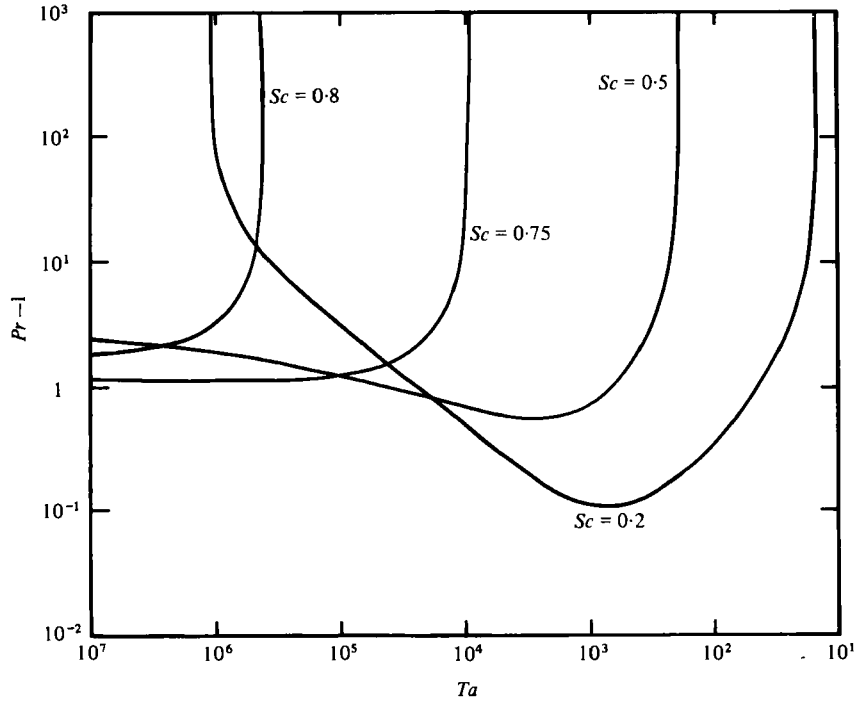

FIGURE 13. Range of Taylor numbers for which multivalued plots exist for fixed Pr and Sc.

sometimes destabilizing effect of a 'stable' density gradient in certain convection problems, including the present problem when $Pr < 1 < Sc$ (discussed in § 3.2*a*). In what follows, we will adapt Acheson's ideas to the situation when Pr and Sc are less than unity.

For small Ta, overstable oscillations can occur when the diffusivities of heat and solute are sufficiently different. The basic overstability mechanism is well understood (Turner 1974). For small Ta, the frequency ω is relatively small so that the parcel can remain in approximate density equilibrium with its environment, *via* the diffusion of heat and solute. As Ta increases, however, so does the oscillation frequency. This has the effect of making it more difficult for the parcel to remain in density equilibrium with its surroundings as it bobs up and down, and the oscillations will grow. Of course, if ω becomes too large, the basic overstability mechanism will fail because very little heat or solute will be transferred to the parcel during a cycle. Thus, we see how instability can be facilitated by an increase in ω, and that if ω is too small or too large, the basic overstability mechanism is not very efficient. Again, as in region II*a*, for some intermediate value of ω, the overstability mechanism achieves its optimal efficiency, and convection becomes possible at a lower value of R_T than is possible for smaller or larger values of ω. This is consistent with the results shown in figure 15, where it is seen that an increase in Ta produces an increase in the non-dimensional group $\omega Pr/y$ (at marginal stability), as well as a minimum in the R_T–Ta plot.

Unlike the problems considered by Acheson, we must account for the diffusion of both heat and solute, so the analysis is slightly different. We find, by analogy to (17),

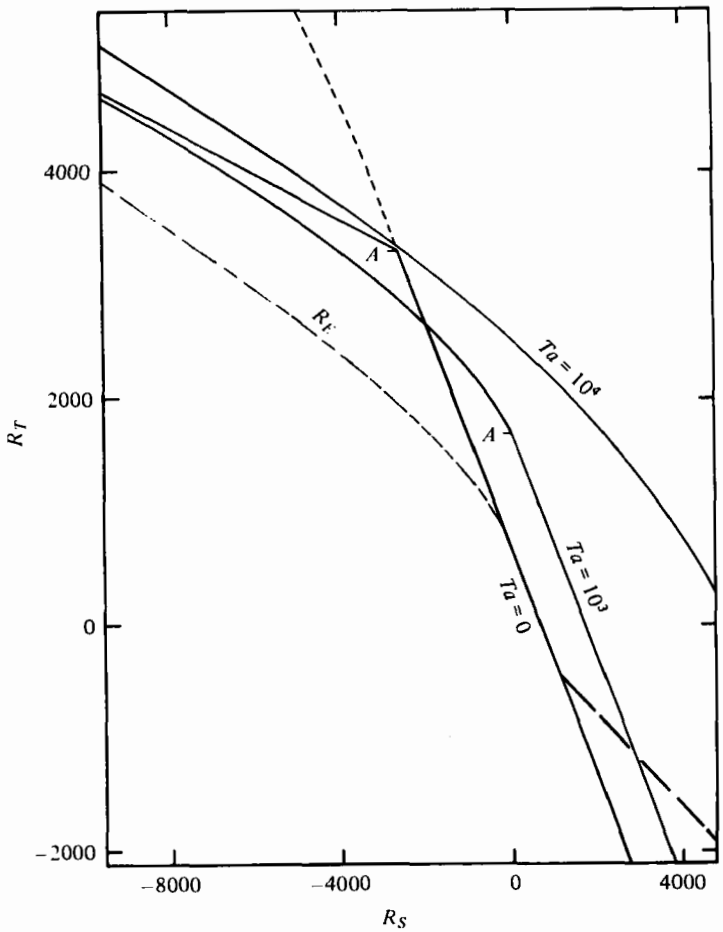

FIGURE 14. Variation of R_T^c with R_S for $Pr = 0{\cdot}2$, $Sc = 0{\cdot}5$. For $Ta = 0$ and $Ta = 1000$, the portion of the stability boundary lying below the slope discontinuity (point A) corresponds to steady onset. The portions of those stability boundaries to the left of point A, as well as the part of the $Ta = 10^4$ stability boundary shown here, correspond to oscillatory onset. The curve labelled R_E is the lower boundary of the region in which Joseph (1970) has shown that subcritical instability is possible for $Ta = 0$. ———, 'Fingering line; – – –, 'diffusive' curve.

the concentration difference between a bobbing parcel and its surroundings as it passes through its equilibrium position to be given by

$$C_A = -h\frac{dC_A}{dz}\frac{\omega Scy}{\omega^2 Sc^2 + y^2} = -h\frac{dC_A}{dz}\frac{\omega Sc/y}{(\omega Sc/y)^2 + 1},$$

where dC_A/dz is the vertical concentration gradient. The corresponding density difference is then

$$\Delta\rho = -\rho_0 hy\left(\alpha_T\frac{dT}{dz}\frac{\omega Pr}{\omega^2 Pr^2 + y^2} - \alpha_C\frac{dC_A}{dz}\frac{\omega Sc}{\omega^2 Sc^2 + y^2}\right),$$

so that the maximum density difference (as a function of ω) occurs when

$$\frac{\partial(\Delta\rho)}{\partial\omega} = 0, \quad \text{which implies} \quad R_T\frac{y^2 - \omega^2 Pr^2}{(y^2 + \omega^2 Pr^2)^2} + R_S\frac{y^2 - \omega^2 Sc^2}{(y^2 + \omega^2 Sc^2)^2} = 0.$$

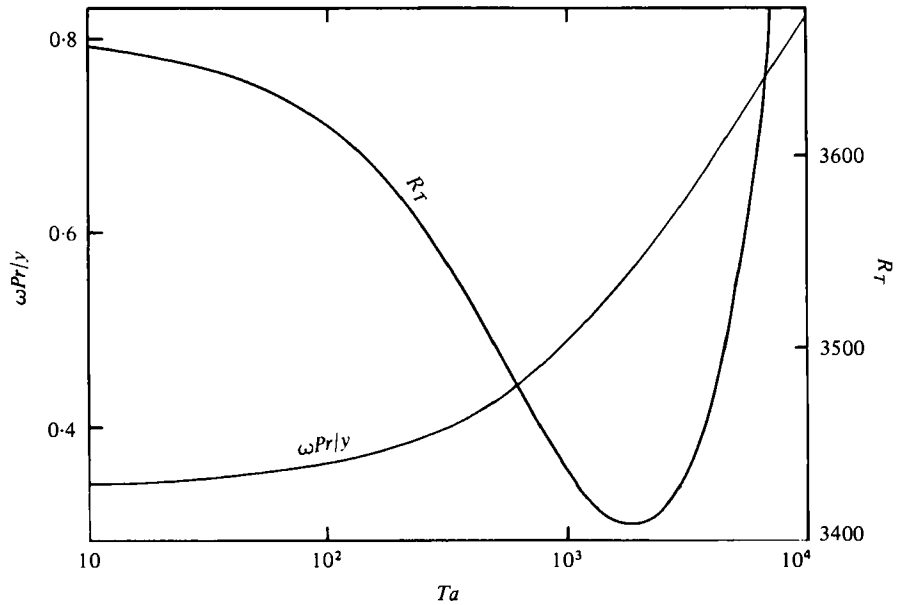

FIGURE 15. Variation of R_T and $\omega Pr/y$ with Ta for $Pr = 0{\cdot}2$, $Sc = 0{\cdot}5$, $R_S = -4500$.

For $Pr = 0{\cdot}2$, $Sc = 0{\cdot}5$, and $R_S = -4500$, substitution of $R_T = 3400$ (the approximate value at the minimum; see figure 15) yields two values of $\omega Pr/y$, namely 0·135 and 1·29, compared with the correct value of 0·57. Given that the analysis only considers the maximization of $\Delta\rho$ at the particle's equilibrium position, this is probably not too bad. In any case, it is clear that the destabilization is associated with an increase in $\omega Pr/y$, and that when $\omega Pr/y$ becomes sufficiently large, rotation again serves to stabilize the layer.

Finally, the energy result of Joseph (1970) is shown as a dashed curve labelled R_E in figure 14. Below this curve, the rotating and non-rotating cases are unconditionally stable. Between this curve and the appropriate (depending on Ta) solid curve, subcritical instabilities are possible. Indeed for several combinations of Pr and Sc in regions IIIa and IIIb, Sani (1965) and Veronis (1968) have demonstrated the existence of subcritical instabilities for $Ta = 0$. These may hinder the experimental observation of the predicted destabilization by rotation in this regime.

4. Discussion and concluding remarks

The principal results of the foregoing *linear* analysis of the stability of a rotating doubly diffusive fluid layer may be summarized as follows.

(i) If the Prandtl and Schmidt numbers both exceed unity, rotation inhibits the onset of motion in both the 'fingering' and 'diffusive' regimes, with the inhibition in the latter being somewhat more pronounced than in the former.

(ii) For $Pr < 1 < Sc$, a rotating layer can be destabilized by the addition of a bottom-heavy solute gradient.

(iii) For $Pr > 1 > Sc$, a rotating doubly diffusive layer can be linearly stable with

a certain temperature gradient, while an identical layer with a less adverse temperature gradient is definitely unstable. The result is that the linearly stability criteria might have to be expressed in terms of three thermal Rayleigh numbers, as opposed to a single 'critical' value.

(iv) For a fluid with both Pr and Sc less than unity, the onset of convection as infinitesimal disturbances in a rotating doubly diffusive layer can occur at a lower adverse temperature gradient than in an identical non-rotating layer.

Whether the interesting predictions of the linear stability analysis summarized above are experimentally realizable depends on the availability of fluids with the proper Prandtl and Schmidt numbers, as well as on the influence of finite amplitude effects and more realistic boundary conditions. With the $R_T \leftrightarrow R_S$, $Pr \leftrightarrow Sc$ invariance understood, binary liquid metals ($Pr \ll 1 \ll Sc$) constitute an appropriate class of fluids for the testing of predictions (ii) and (iii) above. The influence of realistic boundary conditions on the linear stability of a doubly diffusive fluid layer has been studied by Nield (1967), who has shown that the numerical results, but not the qualitative features, are changed. The addition of uniform rotation does not seem likely to alter this conclusion. The question of finite amplitude effects, briefly considered by Sengupta & Gupta (1971), is of special interest, given the existence of subcritical instabilities in both the non-rotating doubly diffusive case (Veronis 1965, 1968; Sani 1965) and the rotating singly stratified case (Veronis 1959).

A necessary condition for the existence in a linear stability problem of the disconnected neutral curves described in § 3.2*b* that give rise to the predictions summarized in (iii) above is that there be a dispersion relation between ω^2 and k that is of degree two or higher in ω^2, or equivalently, that at least two types of wave propagation are possible. Previously studied problems meeting this necessary requirement include the present problem, a rotating fluid layer heated from below in the presence of a magnetic field (Chandrasekhar 1961, chapter V; Eltayeb 1975*a*), a triply diffusive layer (Griffiths 1979), and a viscoelastic layer heated from below and subjected to either rotation (Takashima 1970; Bhatia & Steiner 1972; Eltayeb 1975*b*) or a magnetic field (Bhatia & Steiner 1973; Eltayeb 1976). Disconnected neutral curves actually do occur in the triply diffusive and rotating hydromagnetic layer problems (Pearlstein, unpublished calculations), and might be found in other situations.

The author thanks Professor R. E. Kelly for encouragement and useful suggestions during the course of this work and for several reviews of the manuscript. Dr D. J. Acheson suggested a mechanism to explain the destabilization by a 'stable' solute stratification. Helpful discussions with F. H. Busse, R. M. Clever, S. M. Copley, S. H. Davis, G. Schubert, A. M. Soward, J. M. Straus, and R. K. Ulrich are also acknowledged. Thanks are due to R. L. Sani for supplying a copy of the unpublished work of Sani & Scriven during the course of this investigation. This work constitutes part of a thesis submitted in 1977 in partial satisfaction of the requirements for the M.S. degree in the School of Engineering and Applied Science at UCLA. During this work, the author was supported in part by NSF grants DES 71-00543 and ENG 79-02630, a UCLA Academic Senate grant to Professor Kelly, and an NSF National Needs Graduate Traineeship.

Appendix

For $Pr = Sc$, (14) and (15) may be combined to give

$$R_T^o = -R_S + \frac{2(1+Pr)}{k^2}\left(y^3 + \pi^2 Ta\left(\frac{Pr}{1+Pr}\right)^2\right). \tag{A 1}$$

The minima of (16) and (A 1) are attained when

$$2(k^2+\pi^2)^3 - 3\pi^2(k^2+\pi^2)^2 - \pi^2 Ta = 0 \tag{A 2a}$$

and

$$2(k^2+\pi^2)^3 - 3\pi^2(k^2+\pi^2)^2 - \pi^2 Ta\left(\frac{Pr}{1+Pr}\right)^2 = 0, \tag{A 2b}$$

respectively. Denoting the minimizing values of $k^2+\pi^2$ by $y_s(Ta)$ and $y_o(Ta)$, the corresponding values of R_T^s and R_T^o are

$$R_{T,\,\min}^s = -R_S + 3y_s^2(Ta), \tag{A 3a}$$

$$R_{T,\,\min}^o = -R_S + 6(1+Pr)\,y_o^2(Ta). \tag{A 3b}$$

The determination of linear stability criteria is then reduced to deciding which of (A 3a, b) is the smaller. The preferred mode of instability is independent of R_S, and for fixed Pr, changes from stationary to oscillatory at a value of Ta for which the values of R_T given by (A 3a, b) are equal. It has been shown (Chandrasekhar 1961, chapter III) that there is a Prandtl number $Pr^* = 0{\cdot}67\,660\,498\ldots$ such that

(i) if $Pr > Pr^*$, for all Taylor numbers, the stationary mode is the first to become unstable as R_T is increased and

(ii) if $Pr < Pr^*$, the overstable mode will be observed (according to linear theory) at the lower thermal Rayleigh number if

$$Ta > \overline{Ta} = \frac{27\pi^4(1+Pr-2Pr^2)^2(1+Pr)^{\frac{1}{2}}[(2+2Pr)^{\frac{1}{2}}-1]}{2[(1+Pr)^{\frac{1}{2}}-2\sqrt{2}\,Pr^2]^3}. \tag{A 4}$$

For smaller Taylor numbers, the stationary mode is preferred.

Pr	$\overline{Ta}$	$\overline{Ta}$ (Chandrasekhar)
0	544·70	548
0·1	731·42	728
0·2	1047·0	990
0·4	3132·6	3163
0·5	8500·4	8505
0·55	18837	18870
0·6	67697	68150
0·63	$2{\cdot}5836 \times 10^5$	$2{\cdot}588 \times 10^5$
0·65	$1{\cdot}2463 \times 10^6$	$1{\cdot}223 \times 10^6$

TABLE 2.

The existence of such a critical Taylor number was recognized by Chandrasekhar (1961, pp. 118–119), but the formula (A 4) (obtained by manipulation of (A 2a, b) and (A 3a, b)) appears to have been previously unknown. Values of Ta calculated from (A 4), along with those of Chandrasekhar (1961, table X) are shown in table 2. The latter values, calculated by iteration, are seen to be in error by as much as 5·4 %.

REFERENCES

ACHESON, D. J. 1979 'Stable' density stratification as a catalyst for instability. *J. Fluid Mech.* **96**, 723–733.

ANATI, D. A. 1972 Some evidence of a mesoscale double-diffusivity effect. *Pure & Appl. Geophys.* **96**, 167–170.

ANTORANZ, J. C. & VELARDE, M. G. 1979 Thermal diffusion and convective stability: The role of uniform rotation of the container. *Phys. Fluids* **22**, 1038–1043.

APOSTOL, T. M. 1957 *Mathematical Analysis*. Addison-Wesley.

BAINES, P. G. & GILL, A. E. 1969 On thermohaline convection with linear gradients. *J. Fluid Mech.* **37**, 289–306.

BHATIA, P. K. & STEINER, J. M. 1972 Convective instability in a rotating viscoelastic fluid layer. *Z. angew. Math. Mech.* **52**, 321–327.

BHATIA, P. K. & STEINER, J. M. 1973 Thermal instability in a viscoelastic fluid layer in hydromagnetics. *J. Math. Anal. Applic.* **41**, 271–283.

BRAKKE, M. K. 1955 Zone electrophoresis of dyes, proteins and viruses in density-gradient columns of sucrose solutions. *Arch. Biochem. Biophys.* **55**, 175–190.

CHANDRASEKHAR, S. 1961 *Hydrodynamic and Hydromagnetic Stability*. Clarendon Press.

COPLEY, S. M., GIAMEI, A. F., JOHNSON, S. M. & HORNBECKER, M. F. 1970 The origin of freckles in unidirectionally solidified castings. *Metallurgical Trans.* **1**, 2193–2204.

ELTAYEB, I. A. 1975*a* Overstable hydromagnetic convection in a rotating fluid layer. *J. Fluid Mech.* **71**, 161–179.

ELTAYEB, I. A. 1975*b* Convective instability in a rapidly rotating viscoelastic layer. *Z. angew. Math. Mech.* **55**, 599–604.

ELTAYEB, I. A. 1976 On "Thermal instability in a viscoelastic fluid layer in hydromagnetics". *J. Math. Anal. & Applic.* **54**, 846–848.

GIAMEI, A. F. & KEAR, B. H. 1970 On the nature of freckles in nickel base superalloys. *Metallurgical Trans.* **1**, 2185–2192.

GRIFFITHS, R. W. 1979 The influence of a third diffusing component upon the onset of convection. *J. Fluid Mech.* **92**, 659–670.

HALSALL, H. B. & SARTORY, W. K. 1976 Observations on the stability of sample zones in the zonal ultracentrifuge. *Analytical Biochem.* **73**, 100–108.

HSU, H. W. 1975 Bioseparation by zonal centrifugation. *Separation Science* **10**, 331–358.

JOSEPH, D. D. 1970 Global stability of the conduction-diffusion solution. *Arch. Rat. Mech. Anal.* **36**, 285–292.

LINDEN, P. F. 1974 Salt fingers in a steady shear flow. *Geophys. Fluid Dyn.* **6**, 1–27.

MASON, D. W. 1976 A diffusion driven instability in systems that separate particles by velocity sedimentation. *Biophys. J.* **16**, 407–416.

MASUDA, A. 1978 Double diffusive convection in a rotating system. *J. Oceanogr. Soc. Japan* **34**, 8–16.

NASON, P., SCHUMAKER, V., HALSALL, B. & SCHWEDES, J. 1969 Formation of a streaming convective disturbance which may occur at one gravity during preparation of samples for zone centrifugation. *Biopolymers* **7**, 241–249.

NIELD, D. A. 1967 The thermohaline Rayleigh–Jeffreys problem. *J. Fluid Mech.* **29**, 545–558.

SANI, R. L. 1965 On finite amplitude roll cell disturbances in a fluid layer subjected to heat and mass transfer. *A.I.Ch.E. J.* **11**, 971–980.

SANI, R. L. & SCRIVEN, L. E. 1964 Oscillatory instability of a rotating fluid layer with transfer of both heat and species: linear theory. Unpublished manuscript referred to in Finlayson & Scriven, *Proc. Roy. Soc.* A **310**, 183–219, 1970.

SARTORY, W. K. 1969 Instability in diffusing fluid layers. *Biopolymers* **7**, 251–263.

SCHAAFFS, W. 1975 Rhythmical structures of monomer and polymer systems in rotating diffusion columns. *Prog. Colloid & Polymer Sci.* **57**, 85–93.

SCHECHTER, R. S., VELARDE, M. G. & PLATTEN, J. K. 1974 The two-component Bénard problem. *Adv. Chem. Phys.* **26**, 265–301.

SCHMITT, R. W. & LAMBERT, R. B. 1979 The effects of rotation on salt fingers. *J. Fluid Mech.* **90**, 449–463.

SENGUPTA, S. & GUPTA, A. S. 1971 Thermohaline convection with finite amplitude in a rotating fluid. *Z. angew. Math. Phys.* **22**, 906–914.

STOMMEL, H. & FEDOROV, K. N. 1967 Small scale structure in temperature and salinity near Timor and Mindanao. *Tellus* **19**, 306–325.

TAKASHIMA, M. 1970 The stability of a rotating layer of the Maxwell fluid heated from below. *J. Phys. Soc. Japan* **29**, 1061–1068.

TURNER, J. S. 1974 Double-diffusive phenomena. *Ann. Rev. Fluid Mech.* **6**, 37–56.

ULRICH, R. K. 1972 Thermohaline convection in stellar interiors. *Astrophys. J.* **172**, 165–177.

VERONIS, G. 1959 Cellular convection with finite amplitude in a rotating system. *J. Fluid Mech.* **5**, 401–435.

VERONIS, G. 1965 On finite amplitude instability in thermohaline convection. *J. Mar. Res.* **23**, 1–17.

VERONIS, G. 1968 Effect of a stabilizing gradient of solute on thermal convection. *J. Fluid Mech.* **34**, 315–336.